Hindawi Publishing Corporation
Advances in Acoustics and Vibration
Volume 2009, Article ID 317202, 17 pages
doi:10.1155/2009/317202

Research Article

Dynamic Stability of Cylindrical Shells under Moving Loads by Applying Advanced Controlling Techniques Part I—Using Periodic Stiffeners

Khaled M. Saadeldin Eldalil[1] and Amr M. S. Baz[2]

[1] *Department of Mechanical Engineering, Faculty of Engineering, Tanta University, Sperbay, Tanta, Egypt*
[2] *Department of Mechanical Engineering, University of Maryland, 2137 Eng. Bldg., College Park MD 20742, USA*

Correspondence should be addressed to Khaled M. Saadeldin Eldalil, eldalil01@msn.com

Received 2 April 2009; Accepted 12 July 2009

Recommended by Mohammad Tawfik

The load acting on a cylindrical shell, with added periodic stiffeners, under a transient pressure pulse propelling a pullet (gun case) has been experimentally studied. This study is based on two modes of velocities, the first is subcritical mode and the second is supercritical mode. The stiffeners are added to the gun tube of an experimental gun facility, of 14 mm bore diameter. The radial strains are measured by using high-frequency strain gage system in phase with a laser beam detection system. Time-resolved strain measurement of the wall response is obtained and both precursor and transverse hoop strains have been resolved. The time domain analysis has been done using "wavelet transform package" in order to determine the frequency domain modes of vibrations and detect the critical frequency mode. A complete comparison of the dynamic behavior of the shell tube before and after adding periodic stiffeners has been done, which indicated that a significant damping effect reaches values between 61.5 and 38% for subcritical and critical modes. The critical frequency of the stiffened shell is increased, so the supercritical mode is changed to subcritical mode. The amplification and dispersion factors are determined and constructed; there is a reduction in the corresponding speed frequencies by about 10%. Also the radial-bending vibrations and tube muzzle motions are detected at muzzle velocity ratio of 0.99%, the results indicated that there is a significant improvement in increasing the number of rounds per second by about 36% and increasing the pointing precision by about 47%.

Copyright © 2009 K. M. S. Eldalil and A. M. S. Baz. This is an open access article distributed under the Creative Commons Attribution License, which permits unrestricted use, distribution, and reproduction in any medium, provided the original work is properly cited.

1. Introduction

The analysis of moving loads on elastic structures has drawn the attention of many researchers over the last century. The extent of the efforts dedicated to studying this problem is justified by the wide variety of structures which are subjected to moving loads, such as bridges, gun barrels, rails, work pieces during machining operations, as well as fluid-conveying pipes. In all these structures, the emphasis is placed on studying two basic phenomena. The first phenomenon deals with the amplification of the dynamic deflections caused by the moving loads, as compared with the deflections resulting from the static application of the same loads. The second considered phenomenon is associated with the dynamic instabilities that can be generated when the velocity of the moving loads exceeds certain critical values.

Vibration of gun barrels is one of the most affected because it leads to dispersion of shot patterns. Decreasing dispersion will lead to a more lethal (more likely to hit), survivable (the sooner the enemy is hit the less likely they are to hit you), and sustainable (less rounds need to achieve the desired effect) weapon system. An intuitive way to reduce dispersion is to reduce the vibrations of the barrel. The end of the barrel is the antinode for all vibration modes, so increased exit velocity requirements have led to a demand for longer barrels. Longer barrels are more susceptible to these vibrations, Fryba [1].

Recently, the demand of increasing muzzle velocity arises strongly for defending considerations, so increasing shell length is becoming essential to satisfy the main target together with increasing stability and decreasing weapon mass. These challenging counteractions lead many

investigators to propose theoretical and experimental solutions. The dynamic behavior of cylindrical shells was studied experimentally by Finlayson [2], Simkins [3, 4], Beltman et al. [5], Thomas [6], and Baz et al. [7], the results indicated that increasing bullet velocity by expanding pressure step causing the axisymmetric radial vibration to be several times higher than that produced by the static application of the same load. So, the traveling velocity of the moving load affects the amplitude of the radial response and critical velocity, above which the shell response becomes unstable.

Many authors have been involved with the theoretical determination of the dynamic response of structures subjected to moving loads, Abu-Hilal and Mohsen [8], and Lin and Trethewey [9]. Several theoretical techniques have been considered in order to define the stability limits and conditions for different structures, Nelson and Conover [10], Steele [11, 12], and Bolotin [13].

Ruzzene and Baz [14, 15] studied theoretically the vibrations of cylindrical shells induced by a moving projectile propelled by an internal pressure wave and controlled by placing stiffening rings periodically along the length of the shell. They suggested that the shell response is, therefore, given by the combination of rotationally symmetric and bending motions, which are coupled by the interaction between the moving projectile, the internal pressure, and the shell vibrations. They developed a finite-element model to predict the transient response of stiffened cylindrical shells loaded by a moving projectile propelled by an internal pressure wave. The model is formulated to account for the interaction between moving mass, internal pressure, and shell vibration and to capture the resulting coupling between bending and rotationally symmetric response. Their results demonstrate the capability of periodically stiffened shells of reducing bending vibrations and, therefore, of stabilizing the overall shell response, before and after the projectile leaves the shell. Aldraihem and Baz [16, 17] investigated theoretically the dynamic stability and response of stepped tubes subjected to a stream of moving objects excitations. They found that the stability of certain tube modes can be improved by providing the tube with appropriately spaced steps.

It is obvious that the increased susceptibility of long gun tubes to operation-induced vibration affects precision and accuracy of firing as well as barrel/round interactions during firing. A lightweight, low-cost method is desired to damp firing induced vibrations thereby increasing performance of the gun system. A relatively inexpensive and lightweight method of damping vibrations in some structures is to apply a surface treatment of a stiffening material. The stiffeners are clamped to the base material of the gun tube, in our case. Radial and transverse vibrations in the system result in radial and shear deformation of the stiffening material, which in turn redistribute and dissipate the energy. The presented experimental work provides guidelines and clear vision for the design of gun barrels with increased firing velocity, improved accuracy, and enhanced structural stability.

To the best of our knowledge, investigating the gun tube with added stiffeners as a periodic damped structure has not been investigated experimentally.

This work deals with studying the gun tube with added stiffeners along its length under moving pressure pulse and mass. The length of the shell is about 130 times the caliber (about three times the present practical ratio) and it may increase to double this ratio to account for supercritical dynamics. A gun test facility is constructed, in the "Noise and control laboratory" at the University of Maryland, USA, to account for investigating and measuring the gun dynamics at subcritical and supercritical velocity modes. A complete comparison of the plain and stepped tube is presented. The dispersion and amplification curves are constructed. The configuration of the stepped shell which is chosen herein is quite similar to that of reference [14].

2. Experimental Setup

2.1. Pneumatic 6/12-Feet Gun Tube Facility

2.1.1. Setup Main Components. The experiment was carried out with in-door helium gun in the vibration and noise control laboratory at University of Maryland, it has a stainless steel tube length of 6 feet, and can be extended to the similar length in the case of running supercritical bullet velocities, as discussed in details by Baz et. al. [7]. Figure 1 shows schematic diagram of the gun system components and Figure 2 shows a view picture of the test setup facility.

As shown in Figure 1, the gun facility is composed of four main parts as follows.

Part 1: pullet decelerator (1),

Part 2: stainless steel tube assembly (2, 14),

Part 3: pneumatic gun machinery (3, 4, 6, 7, 8, 9, 10, 11, 12, 13),

Part 4: firing control box (5).

All the four mentioned parts are assembled on the main base structure (15).

2.1.2. Shooting Mechanism. The bullets are installed in the magazine (3) in Figure 1 and the system power supply is turned on (115 v ac). When Turning "ON" the firing switch in the control box, the air will permit to feed the main and booster cylinders (11) and (6) by low air pressure (220 psi). This will make their push rods to proceed forward to release one bullet from the magazine end and move it to the front of the gun core (12). When the bullet attains this location, a pulse of high-pressure helium will applied on the back of it, then it starts to move through the accelerator (13) which has sloped inlet bore and smaller diameter than the bullet at the rest of it, as shown in Figures 3(a) and 3(b). Due to this diameter difference, the bullet will be extruded and the helium pressure starts to grow up to almost near its maximum value. At this moment, the pressure forces will release the bullet by very high acceleration value. The

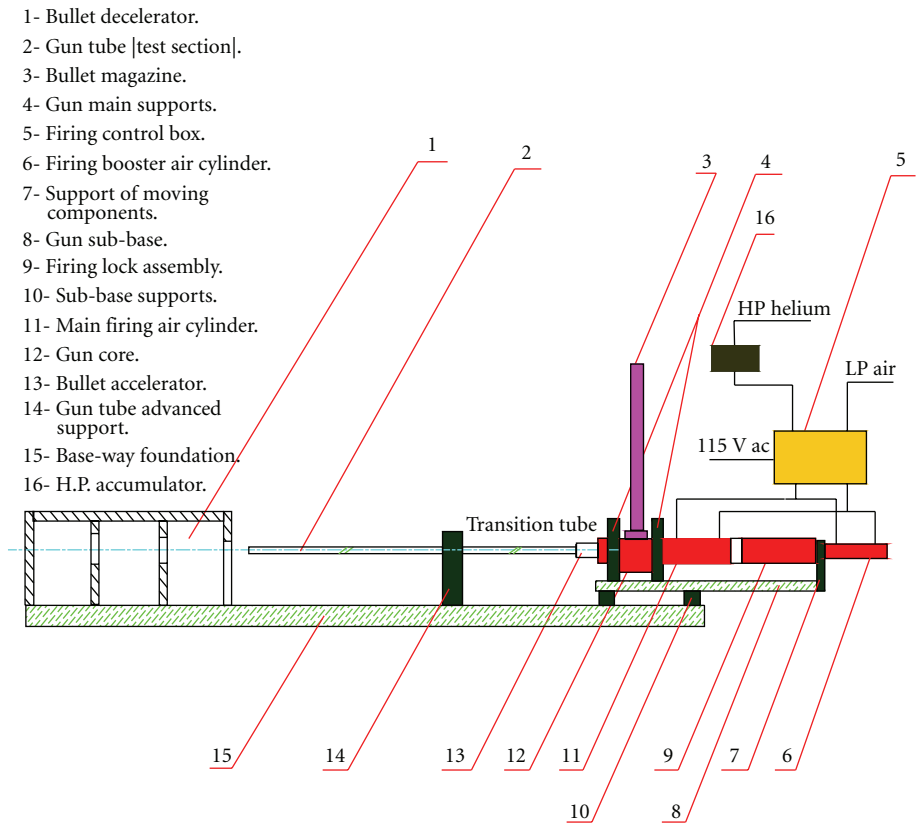

Figure 1: Experimental layout.

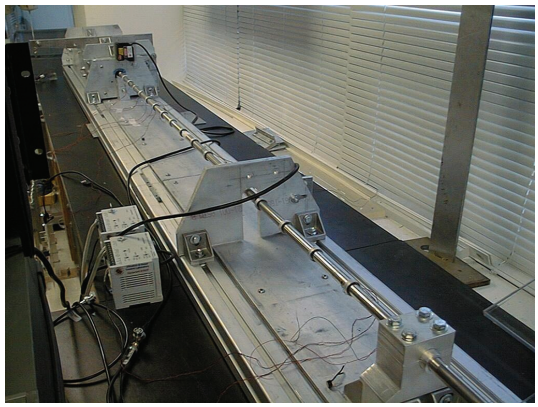

Figure 2: Setup view picture.

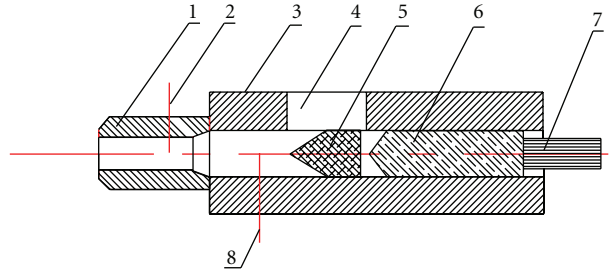

(a) The bullet comes inside gun core

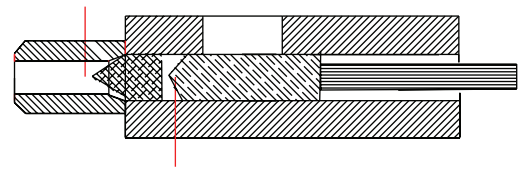

(b) The piston moves the bullet forward

Figure 3: Scheme of shooting mechanism.

high-pressure accumulator is used to keep the pressure pulse almost constant during the firing operation until the bullet leaves the muzzle.

After the bullet comes out from the gun tube, the feeding air of the cylinders will reverse and the piston rods will move back to their original positions. When the firing switch is on single shooting position, the piston will stay at its original location but if the firing switch is on automatic position, the shooting cycle will be repeated until the magazine will get empty. The kinetic energy of the bullet will be absorbed in the decelerator box (1). It partitioned to several rooms containing layers of foam sheets and its walls are made from hard aluminum of 0.5″ thickness.

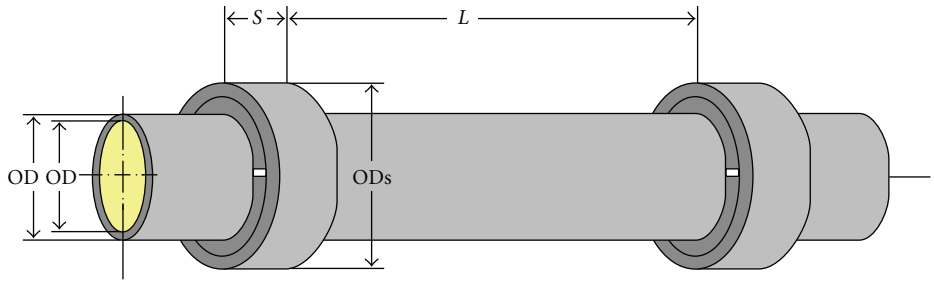

Figure 4: Tube-stiffeners configuration.

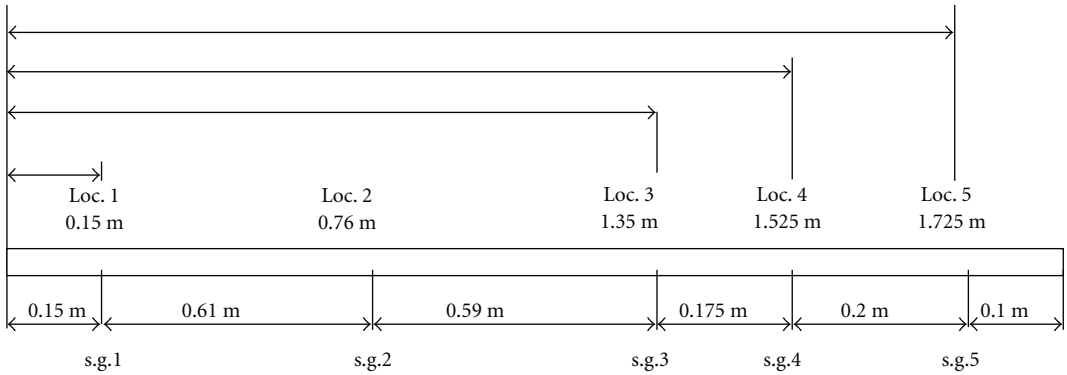

Figure 5: Measuring point locations on the plain and stepped gun tube for subcritical velocities.

2.1.3. Experimental Measurements. The gun tube is made from stainless steel; it has inner and outside diameters of 14.097 and 15.113 mms. The tube has a length of 1830 mms (130 times the caliber); it may be fixed directly on the bullet accelerator outlet or to the end of transition tube (another 130 caliber) at the advanced support (14) as shown in Figure 1. The transition tube is used to extend the expansion process and get supercritical bullet velocities and it has the same length and inner diameter as the gun tube but the outside diameter is bigger. The gun tube is supported as clamped-free to account for bending vibration response and as clamped-simple for radial vibration response measurements.

Five Micro Measurements strain gages of type "CEA-09-062UW-350" and signal conditioning amplifier were used to record the transition response of the gun tube. The strain gages were located at 150 (number 1), 760 (number 2), 1350 (number 3), 1525 (number 4), and 1725 (number 5) mms from the tube inlet, as shown in Figure 5. When extending the gun tube for supercritical measurements, we use only three strain gages locations, they are numbers 1, 4, and 5, as shown in Figure 19. The strain gages were mounted to measure the circumferential strains on the gun tube surface, so it adhered in a perpendicular direction to the tube axis.

The average steady-state deformation strain and the position of the bullet are measured by hand-made piezoelectric foil transducers of type PVDF film, adhered on the gun tube outside surface, and located at the same location plane of the strain gages but at orientation angle of 90°. The ac. signals are rectified by using full wave rectifier and displayed directly without any modulations. The average velocity of the bullet is obtained by measuring the strain gage signals and at the point just ahead of it (e.g., 1 and 2, then 2 and 3, etc.), the time difference between two consecutive points is measured and the distance is known, so, the average velocity is estimated. Also in order to confirm these results by additional measurements, a laser beam analog sensor is located at the outlet of the gun tube.

2.1.4. Experimental Procedure. The experiment was first done for gun tube free from stiffeners (plain tube) and a basic reference is completed and confirmed by many trails at the same conditions (pressure, bullet size, and weight). The experiments were done when the gun tube is evacuated at short and double tube length, in order to obtain low (subcritical) and high (supercritical) bullet velocities.

2.1.5. Controlling Stiffeners. The control stiffeners are used to redistribute and dissipate the energy of the structure. Its optimum number and size is chosen similar to that theoretically studied in [14]. The size of the stiffener is $S = 3.175$ mms long, outside and inside diameters (OD and ID) are 20.828 and 15.113 mms. The stiffener is composed from two part, outer ring and inner two half rings. The numbers of stiffeners were found to be 17 and the distance apart is $L = 100$ mms. The weight of the total stiffeners (the mass added to the gun tube) is found to be 23.32 g, about 5.6% of the tube weight. Figure 4 shows the shell stiffeners configuration.

2.1.6. Critical Parameters Prediction. The projectile critical velocity may be estimated by the followin expresion [18]:

$$V_{\text{cr}} = \sqrt{\frac{Eh}{\rho R}}\left[\frac{1}{3(1-\nu^2)}\right]^{0.25}, \quad (1)$$

where E: Young's modulus of elasticity of the tube; H: tube wall thickness; ρ: denesity of the tube material; R: tube average radius; ν Poisson's ratio of the tube material.

The critical radial frequency for infinite length for thin shells of thickness to radius ratio is less than 1/30 may be estimated with reasonable accuracy according to the findings of Baron and Bleich [19, 20] and Tang [21]:

$$\omega_{\text{cr}} = \frac{K}{a}\sqrt{\frac{Gh}{m}}, \quad (2)$$

where G: shear modulus $= E/2(1+\nu)$, N/m^2; m: mass of shell per unit of area $= \rho h$, kg/m^2; K: factor, $= \pi a/L$ in case of fundamental frequency $n = 0$, L: half wave length, m; a: tube mean diameter, m, then

$$\omega_{\text{cr}} = \frac{K}{a}\sqrt{\frac{E}{2.6\rho}}\ \text{rad/s}. \quad (3)$$

The estimated critical frequency will be 11462.5 Hz, also the value of the critical radial frequency is the same as estimated by [18].

3. Experimental Results and Analysis

3.1. Subcritical Case. The measurements were taken at five locations on the gun tube of length 1.825 m (130 calipers), as shown in Figure 5, for plain and with 17 single stiffeners.

3.1.1. Plain Tube Measurements. Samples of the time domain measurements of plain tube at location points that are specified before are shown in Figures 6(a), 6(b), and 6(c).

As stated in [7], the projectile velocity at location number 1 is very low (about 85 m/s) and the pressure puls is at its maximum value of 1600 psi. The resulting vibration is due to the detonation effect (sudden pressure rise) of the compressed helium at the intry of the accelerator chamber. The obtained vibration is considered as a radial circumference flextural mode (6.8 kHz), Blevins [18]. At location number 2, the velocity is increased to 515 m/s and the pressure value starts to become almost constant due to controlling the rate of injected Helium to be balanced with its expansion rate.

At location number 3, the velocity is increased to 810 m/s, and became about 80% from the theoretically calculated critical velocity (1045 m/s) so the radial vibration frequency increased and the radial deformations started to grow up. The amplification (ε) factor (normalized amplitude) became more than unity and its value can be calculated by

$$\varepsilon = \max \cdot \text{strain/Lame deformation}. \quad (4)$$

At location number 4, the projectile velocity reaches 917 m/s, that is, 88% and the head frequency is increased to 92 kHz and trailing wave became about 120 kHz. As the projectile proceeds toward the tube muzzel, the velocity increases to 980 m/s at location number 5 and the head wave frequency is found to be 80 kHz and the trailing wave reached to 145 kHz. These variations in the wave frequency, which decrease the

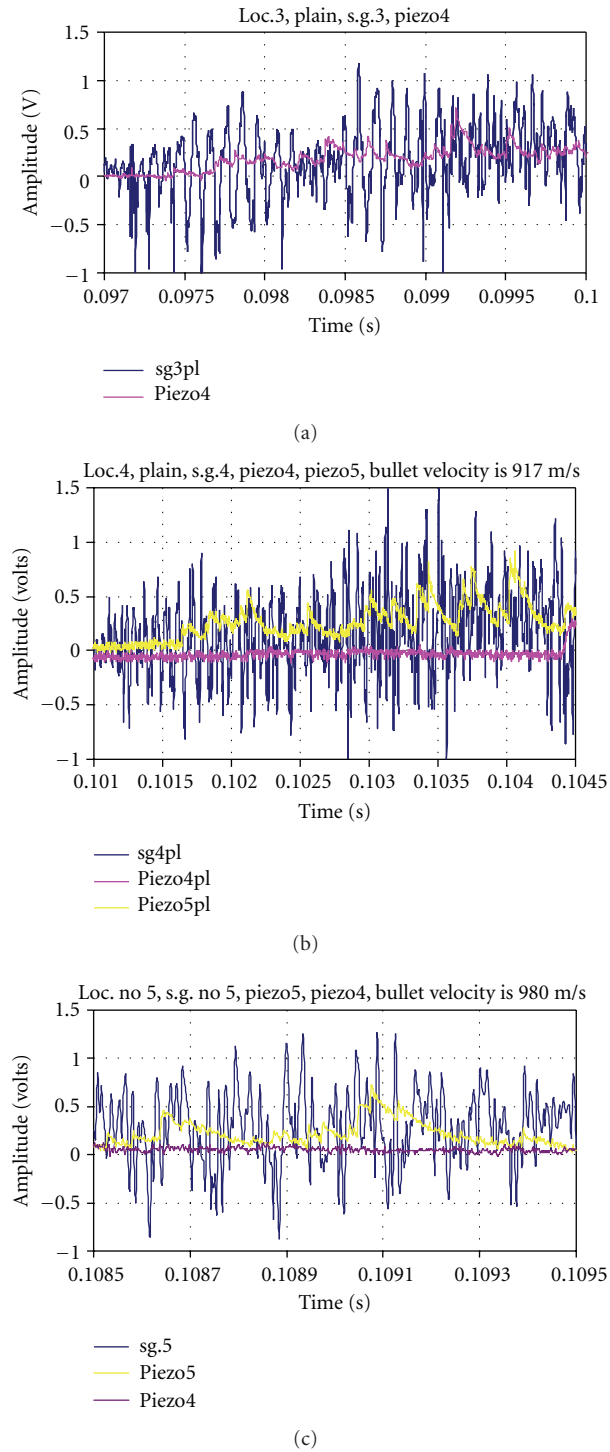

Figure 6: (a) Time domain output at location number 3. (b) Time domain output at location number 4. (c) Time domain output at location number 5.

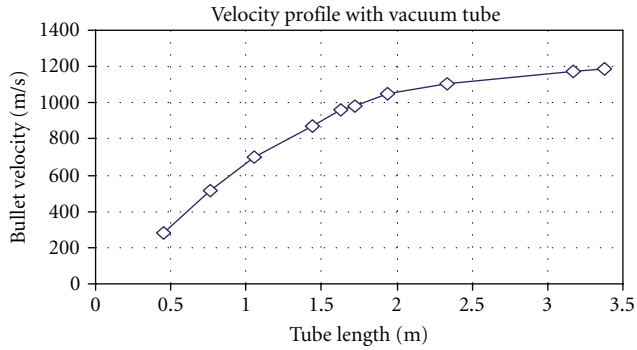

Figure 7: Bullet velocity profile with vacuum for tube length of 260 calibers at pressure pulse of 1600 psi.

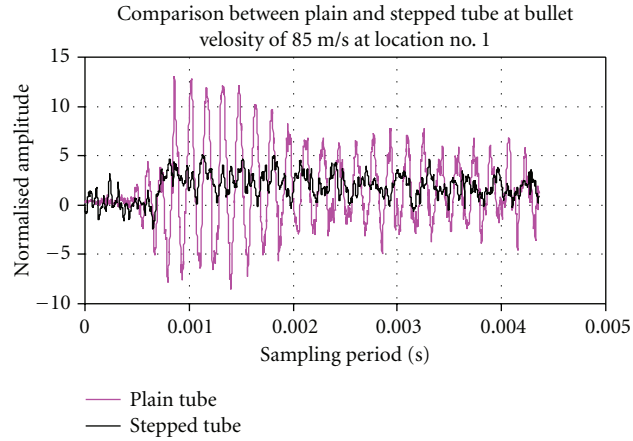

Figure 8: Comparison time domain measurements at location number 1.

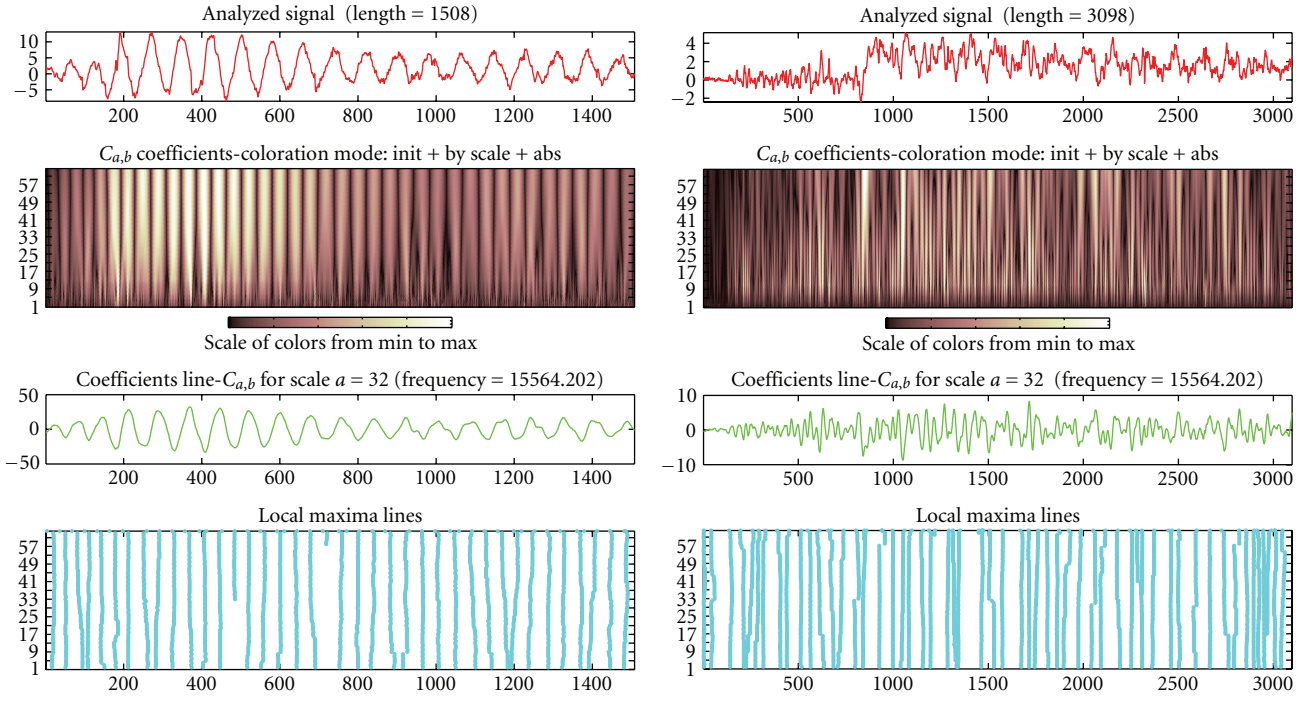

(a) Plain tube (b) Stepped tube

Figure 9: Time-frequency representation at location number 1.

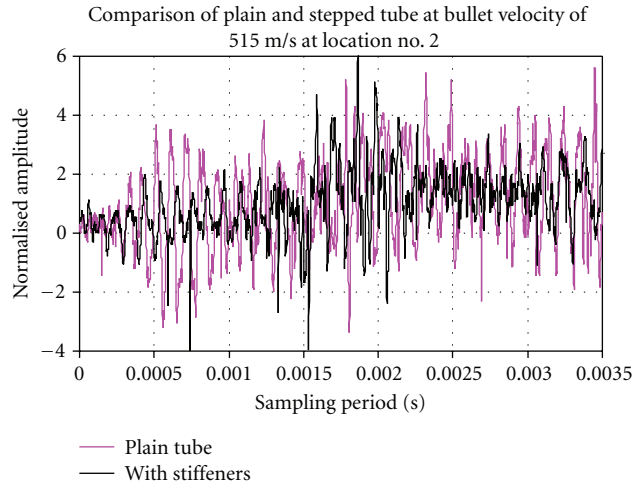

FIGURE 10: Comparison of time domain measurements at location number 2.

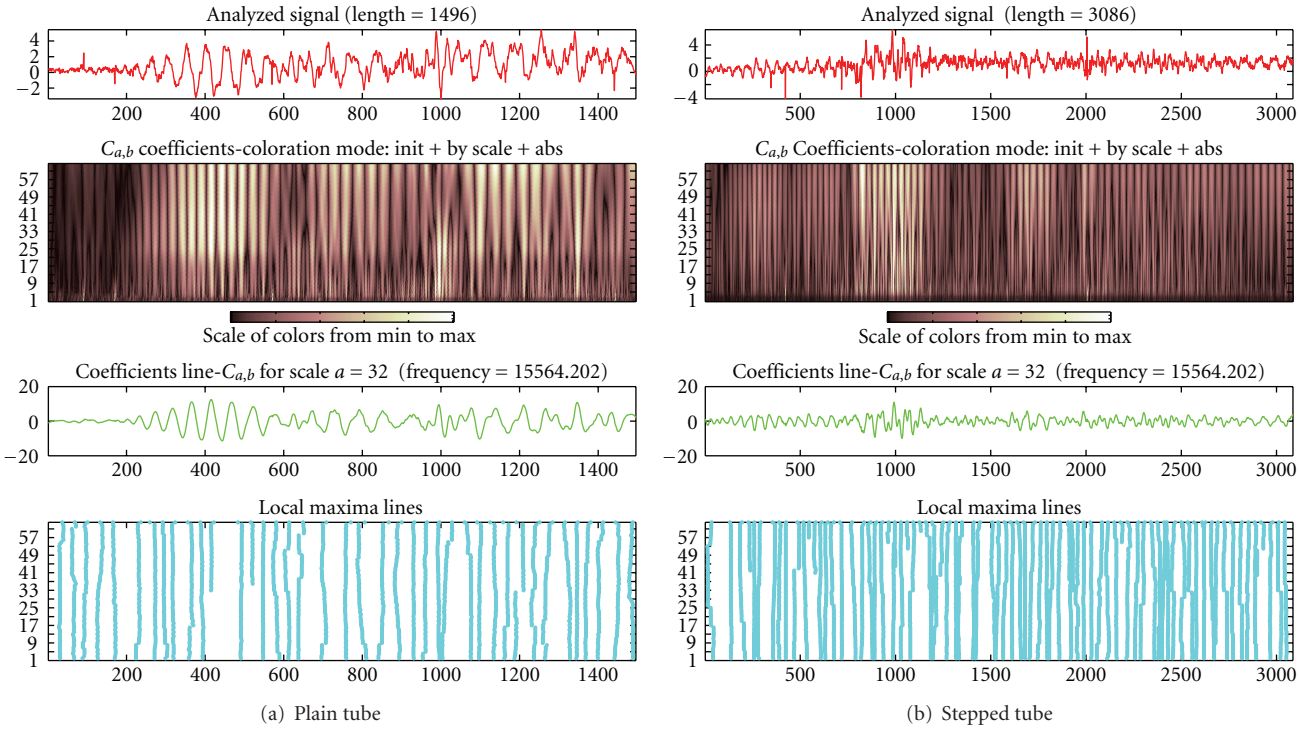

(a) Plain tube (b) Stepped tube

FIGURE 11: Time-frequency representation at location number 2.

head wave and increase the trailing wave, extrapolate that the critical velocity may be happening. The projectile leave the tube muzzle at a velocity of about 1015 m/s, that is, 97% of the critical velocity. So, some very large deformations occurred at the tube muzzel due to these transient transformation to the critical case. The velocity profile of the bullet inside a vacuum tube is shown in Figure 7. The avarage static deformation (Lame deformation) is found to be equal to the equevelant output strain voltage of 0.25 v.

3.1.2. Shell with Added Stiffeners Measurements. A comparison time domain measurements of the shell after adding stiffeners to its surface at the same location points, which are specified before, are shown in Figures 8, 10, 12, 14, and 16. The amplitude is normalized according to the L'me deformation and the time is shifted to starts from zero.

The effect of adding stiffeners is found to be significant. At location number 1 (Figure 8), where the low frequencies are the most, the amplification is reduced by 61.5%. The

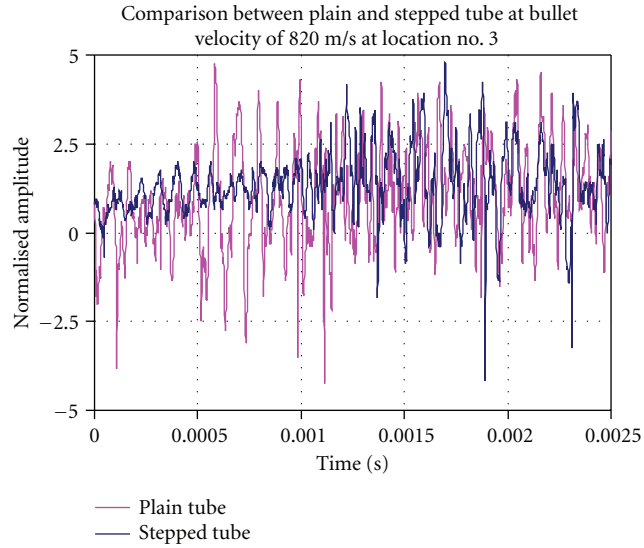

Figure 12: Comparison of time domain measurements at location number 3.

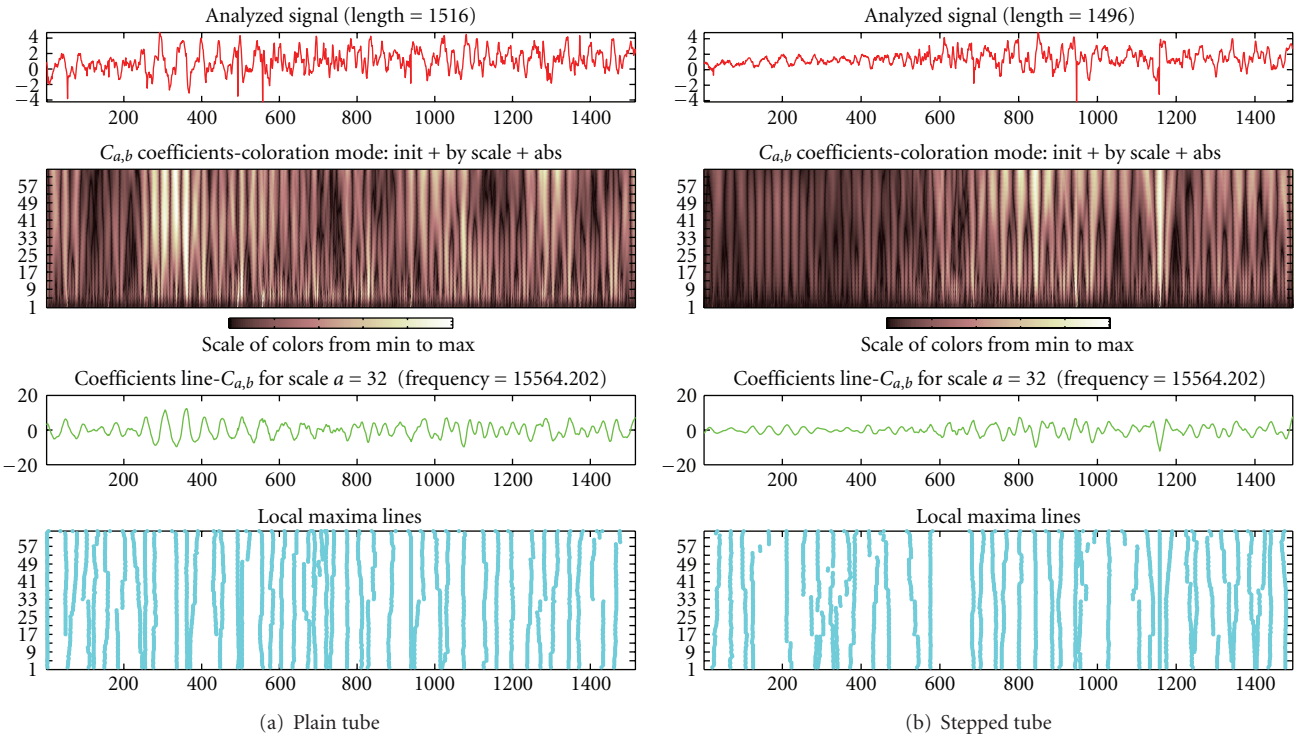

(a) Plain tube (b) Stepped tube

Figure 13: Time-frequency representation at location number 3.

shape of the strain signal is transferred to a classical subcritical signal shape. The same effect is continued at all the subsequent four locations; as shown in Figures 10, 12, 14, and 16. At locations numbers 2 and 3, the frequency starts to increase, so the total period of the signals is suppressed in shorter time. The stiffened tube amplification factor is decreased by 20% at locations numbers 3 and 4 and by 38% at location number 5.

The frequency analysis have been done using "wavelet transform (WT)" instead of "fast Fourier transform (FFT)" in order to detect the stronger high frequency modes which are built-in with the resulting vibrations. The ability of the wavelet transforms to detect very high frequencies is due to its very narrow scanning window (time span) which may be equal to the sampling period, so, it can deal well with the dynamic waves and the signal decomposition will be

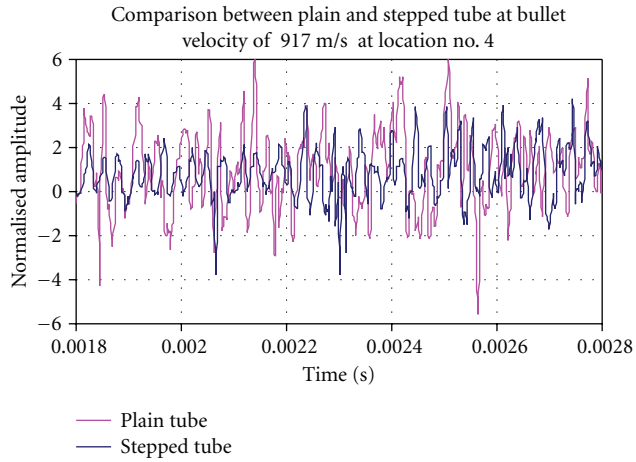

Figure 14: Comparison of time domain measurements at location number 4.

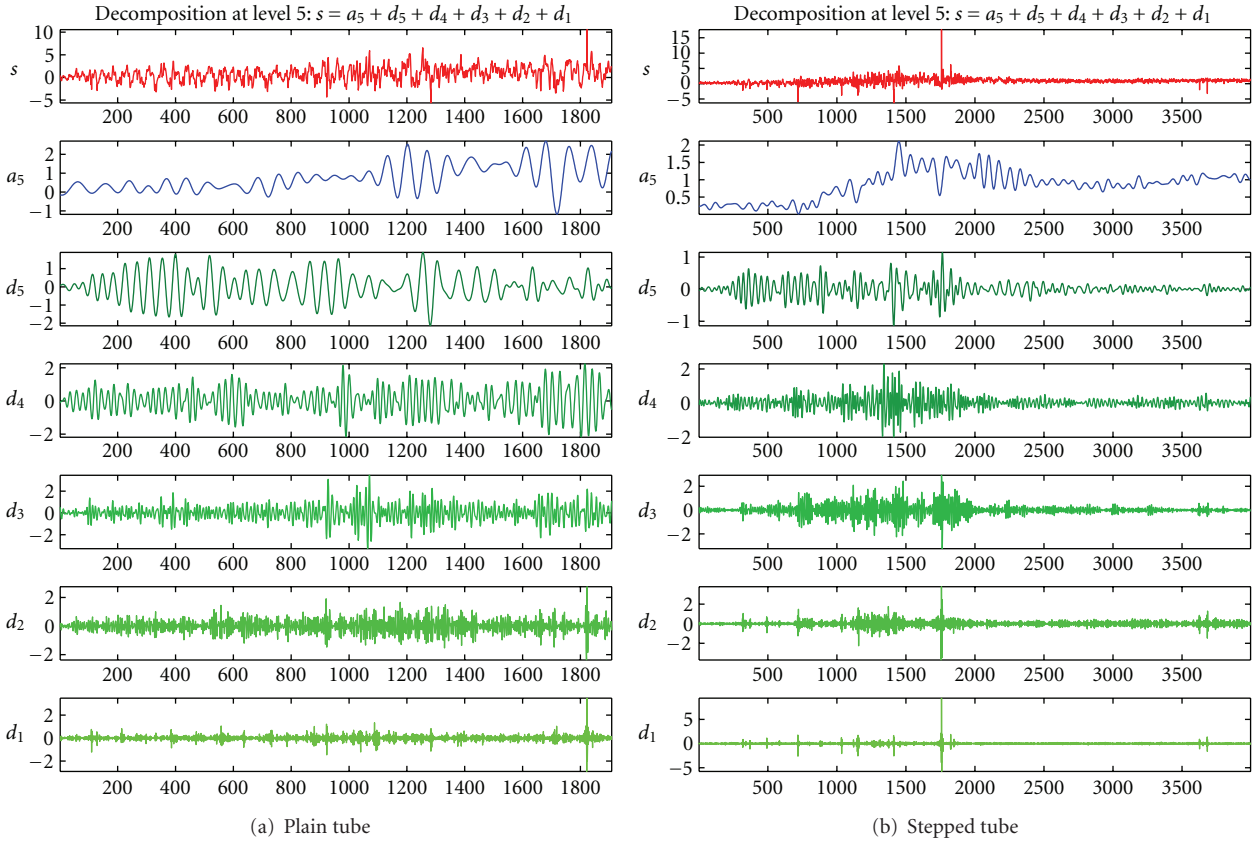

Figure 15: Time-frequency representation at location number 4.

obtained perfectly. Also the wavelet transform gives frequency modes corresponding to its time domain locations, so the interfering noise could be avoided which may be prevent any confused results.

Contrarily, the fast Fourier transform has a wide scanning window, so it detects only stationary signals which have limited frequency changes over long periods. Also, the frequency and time information of a signal at some certain point in the time-frequency plane cannot be known. In other words, we cannot know what spectral component exists at any given time instant, so the analysis will comprise trickery results.

A comparison of the time-frequency decomposition domains is illustrated in Figures 9, 11, and 13 at locations numbers 1, 2, and 3, respectively. The figures indicate that the frequency domain appears as a colorization area (pink color),

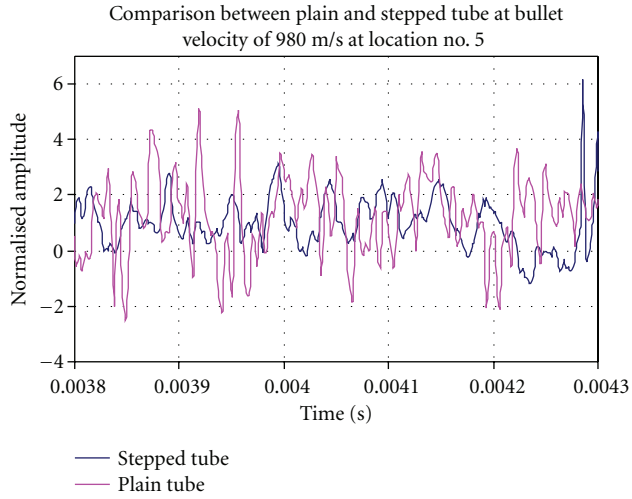

Figure 16: Comparison of time domain measurements at location number 5.

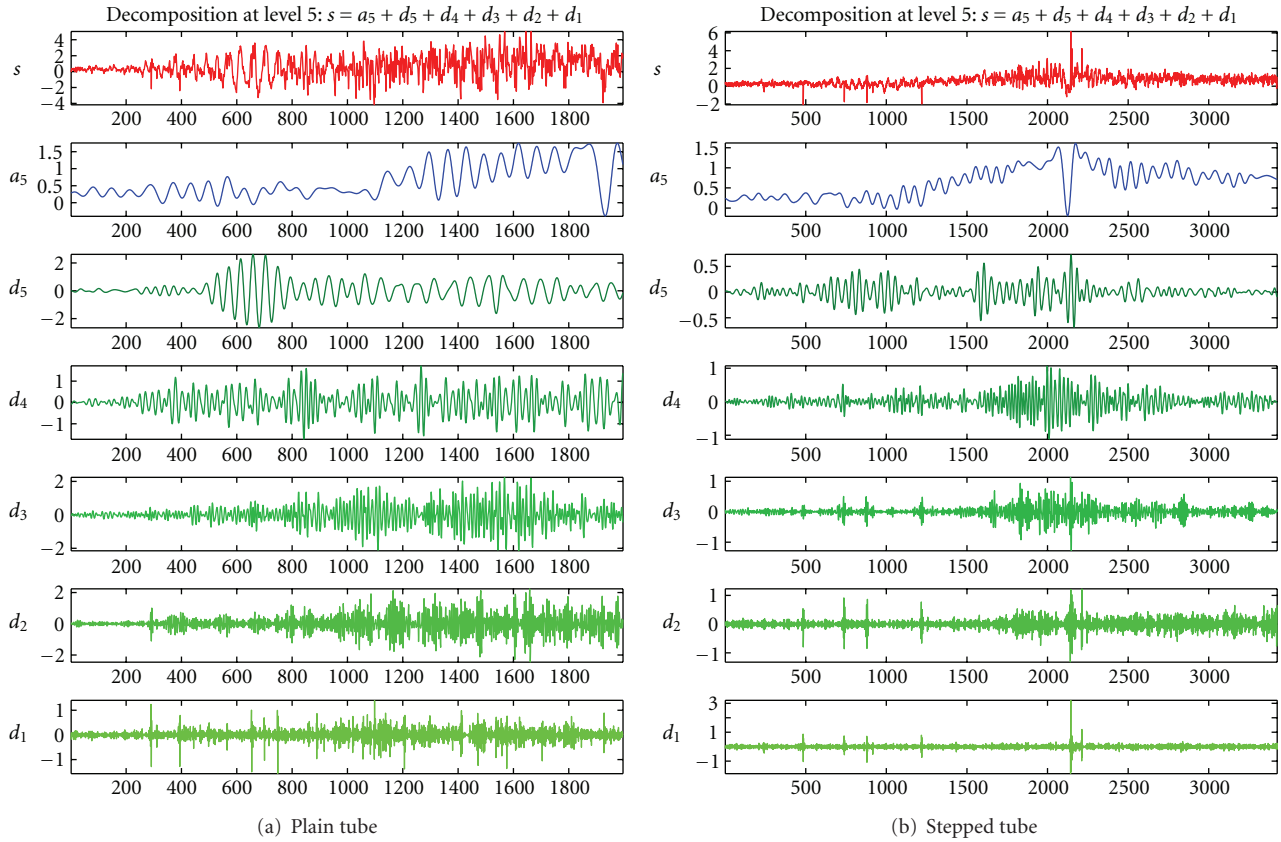

(a) Plain tube (b) Stepped tube

Figure 17: Time-frequency representation at location number 5.

it changes from dark to bright as the amplitude increases from minimum to maximum; also the frequency is defined by a so-called parameter "Scale" which is proportional to the inverse of the frequency multiplied by a certain factor depending on the used decomposition function of WT family. The figures indicate that the high frequency modes are suppressed due to using stiffeners; also they indicate that the frequency modes decomposition is carried out corresponding to its time domain location.

Figures 15 and 17 show the results of signal processing (decomposition) at locations (4 and 5) by using discrete wavelet transforms. The modes herein are called coefficients, a_1 represents the most very lower frequency mode. The higher frequency modes are represented by coefficients d_5 to

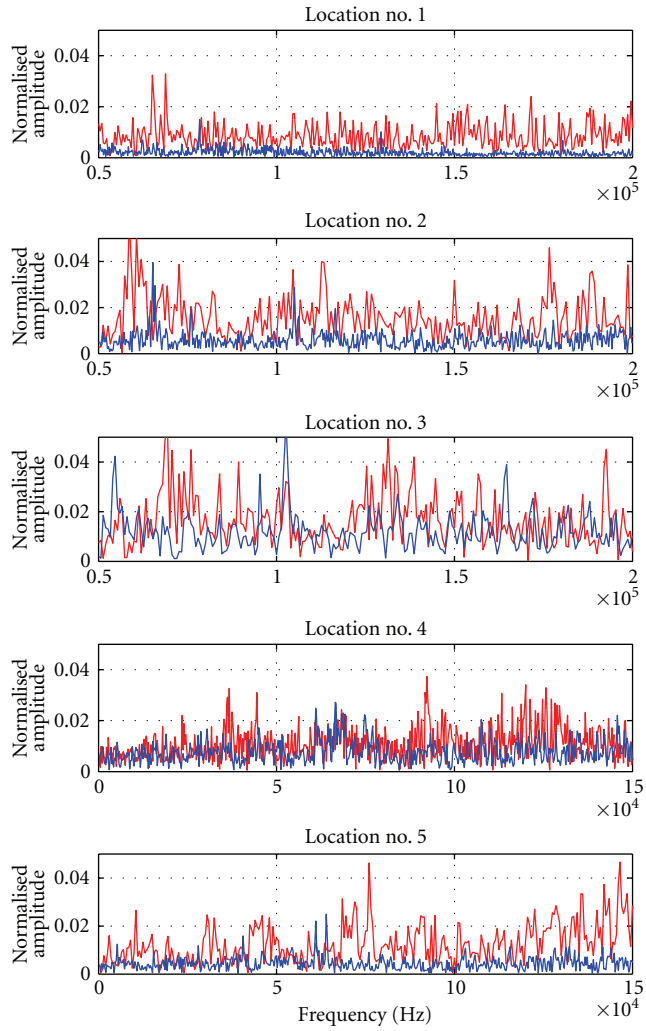

Figure 18: Frequency-domain analysis at locations 1, 2, 3, 4, and 5, red color for original and blue color for stepped tube.

d_1 (from low to high). It is obvious, from the figures, that there is higher amplitude frequencies for coefficients d_3, d_2, and d_1 in the case of plain tube, but these corresponding coefficients are suppressed to lower amplitude values in the case of stepped tube.

Figure 18 shows a comparison of the frequency domain analysis at the five mentioned tube locations before and after using stiffeners. The figure indicates that the absolute value of the signal amplitude is increased at locations numbers 4 and 5, where the critical and supercritical symptoms are started.

3.2. Supercritical Measurements. As mentioned earlier, the supercritical measurements are taken with the aid of extension tube, which is similar to the subcritical tube in length but it has double wall thickness. This double wall thickness tube has higher values of critical velocity and frequency, so, running the experiment will be safer and its damage will be avoided.

3.2.1. Plain Tube Measurements. The measurement locations are shown in Figure 19. Samples of the obtained supercritical measurements are shown in Figures 20(a) and 20(b) at locations numbers 6 and 8.

At location number 6, the velocity was found to be 1050 m/s, that is, about 100.5% above the critical velocity. The signal shape is resembles the classical super critical signal of [4]. At locations number 7, the signal amplitude is decreased but the velocity increased to 1176.5 m/s, then at location number 8, the velocity increased to 1190 m/s, about 113.9% of the critical velocity and the frequency amplitude continued in decreasing.

At location number 7, the detected frequency of the head wave is found to be 70 kHz, and the trailing wave is 155 kHz and at location number 8, the trailing wave frequency is found to be more than 200 kHz.

3.2.2. Shell with Added Stiffeners Measurements. A comparison of the time domain measurements of plain and stiffened tube are shown in Figures 21(a), 21(b), and 21(c). The amplification factor at location number 6 is decreased to a value of 25% of that obtained of the plain tube, and the signal shape is changed to be as a typical classical subcritical

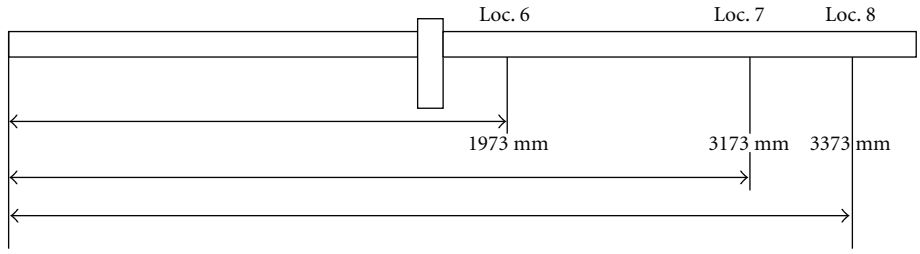

Figure 19: Supercritical measuring locations.

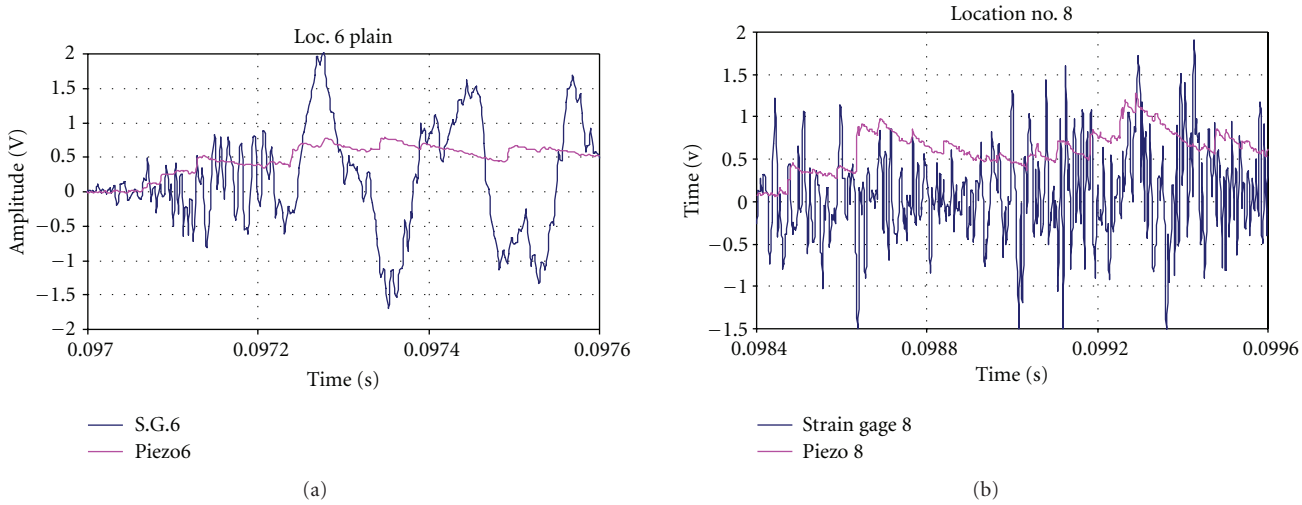

Figure 20: (a) The output signals at location 6, plain tube. (b) The output signals at location 8, plain tube.

shape, that is, the supercritical condition is transferred to subcritical case. At location number 7, the amplitude of the high frequency of the stiffened tube is increased by about 90% of that of the plain tube, this is due to increasing the bullet velocity and frequency. At location number 8, the amplification factor is increased to about 100% than that of the plain tube.

The signal decomposition diagrams at locations numbers 6, 7, and 8 are shown in Figures 22, 23, and 24. The figures show that the amplitude of vibrations at location number 6 of coefficients d_2 and d_1 are decreased due to using stiffeners, it is just aft-critical location. The component d_1 of the stiffened tube is reduced or almost vanished. The high-frequency mode amplitude d_2 of the stiffened tube at locations number 7 is started to increase together with the head wave frequency and continued increasing at location number 8 where it includes the vibration modes of d_2 and d_1.

The frequency domain analysis of the high-frequency modes for both plain and stiffened tube (d's coefficients), at the corresponding measurement locations, are shown in Figure 25. The figure indicates that the supercritical appearance at location number 6 is transformed into subcritical mode by using periodic stiffeners. Contrarily, the critical and supercritical symptoms are obviously started at locations numbers 7 and 8 of the stiffened tube.

The amplification factor diagram is shown in Figure 26, it is obvious that the stiffened tube frequencies are shifted to lower values than the plain tube by about 10%, and the critical velocity is increased to about 1190 m/s. The dispersion curve is constructed and shown in Figure 27, the figure indicates that the expected critical frequency is 114 kHz and the critical velocity is 1045 m/s for the case of plain tube, as obtained by [18–21]. The critical velocity and critical frequency is increased, in the case of using stiffeners to about 1190 m/s and 200 kHz, respectively. So, adding stiffeners to the plain tube leads to increasing the critical velocity and frequency.

3.3. Measurements of Radial-Bending Vibrations. The radial-bending vibrations of plain and stiffened tube are shown in Figures 28 and 29. The tube support is changed to clamped-free, while in the previous study, it was clamped-simple. It is obvious that the stability time which the tube walls taken to rebound is decreased in the case of stiffened tube from 140 ms to 90 ms, by a ratio of about 36%. So, this will lead to increasing the number of rounds from 7 to 11 rounds per second with good retargeting precision.

3.4. Measurements of Tube End Traverse Pointing Motion. The motion of the gun tube end is very important to satisfy

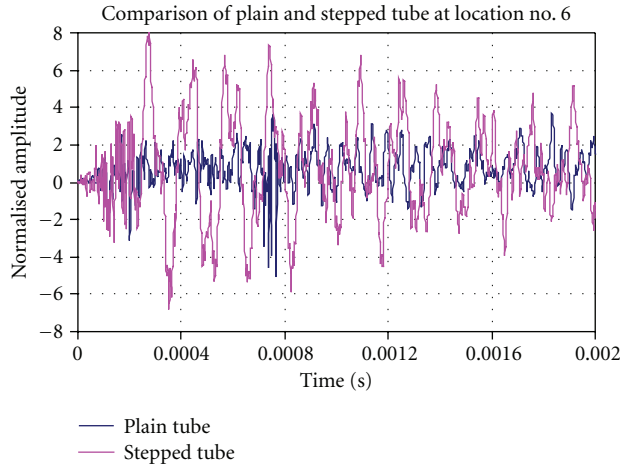

(a)

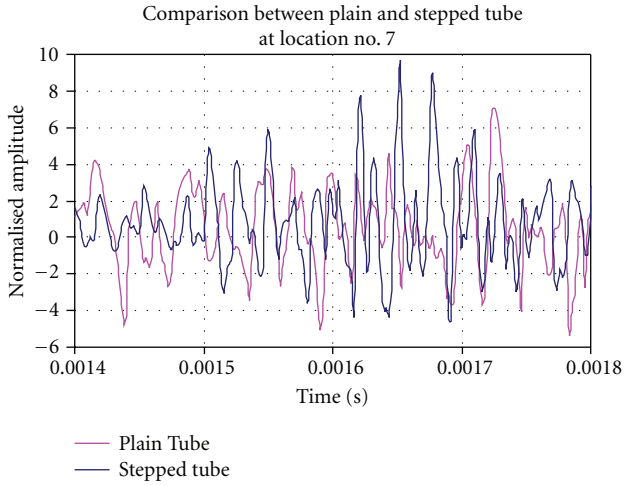

(b)

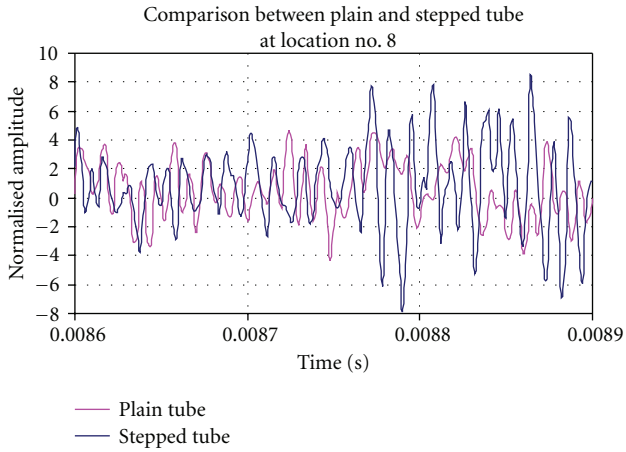

(c)

Figure 21: (a) Comparison of time domain measurements at location number 6. (b) Comparison time domain measurements at location number 7. (c) Comparison of time domain measurements at location number 8.

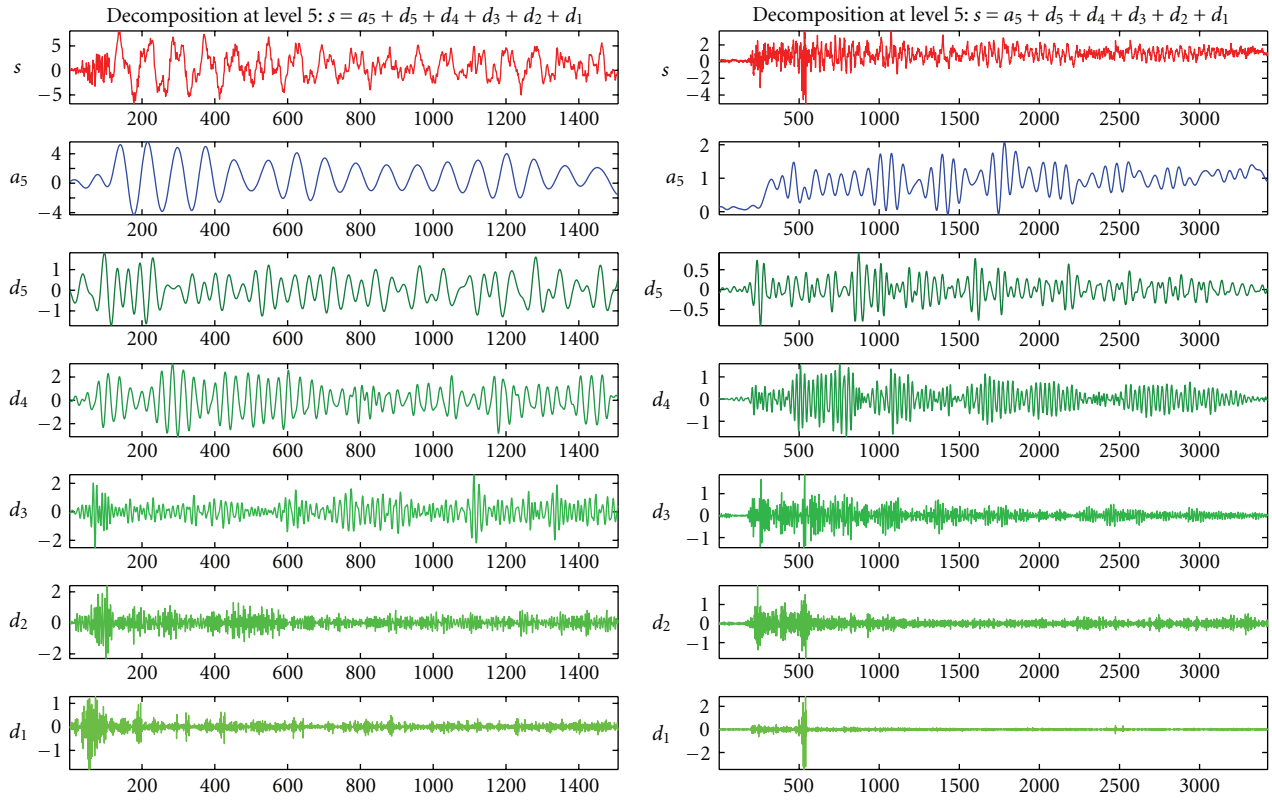

(a) Plain tube (b) Stepped tube

Figure 22: Strain signal decomposition at location number 6.

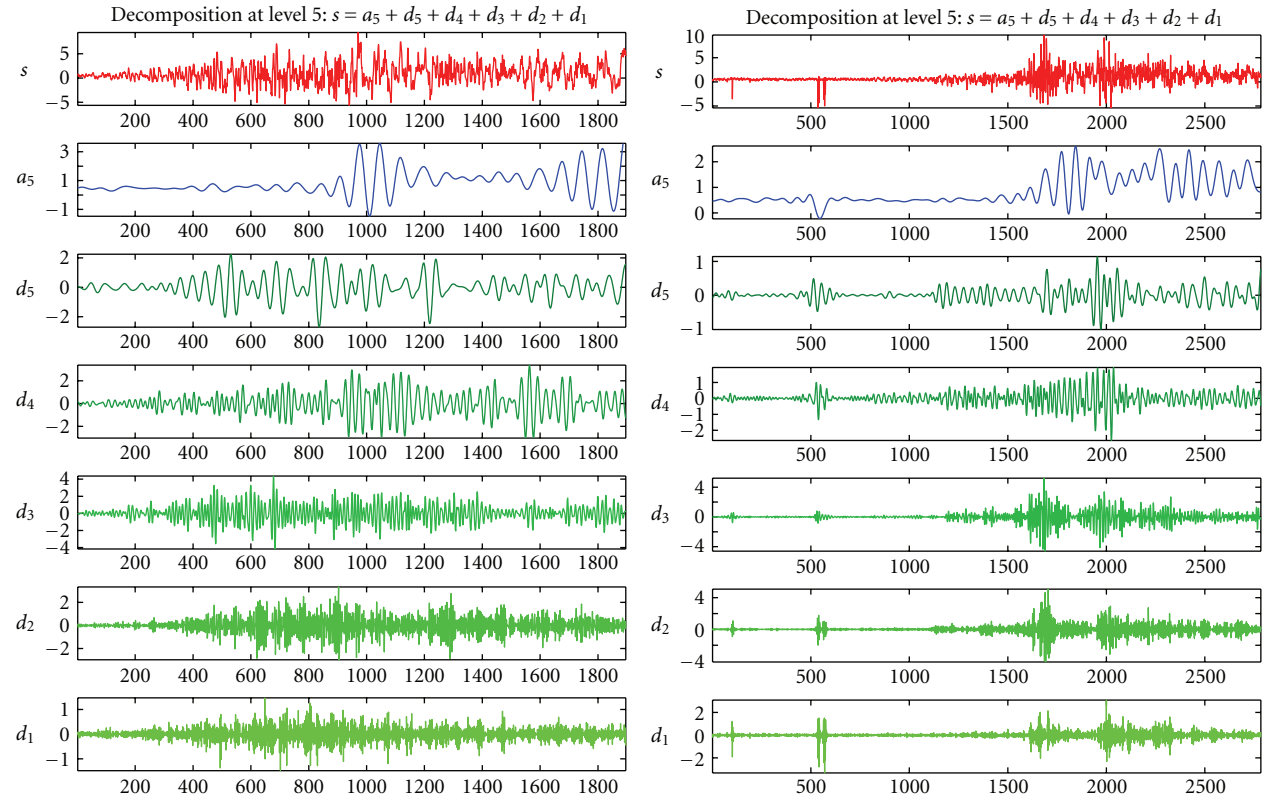

(a) Plain tube (b) Stepped tube

Figure 23: Strain signal decomposition at location number 7.

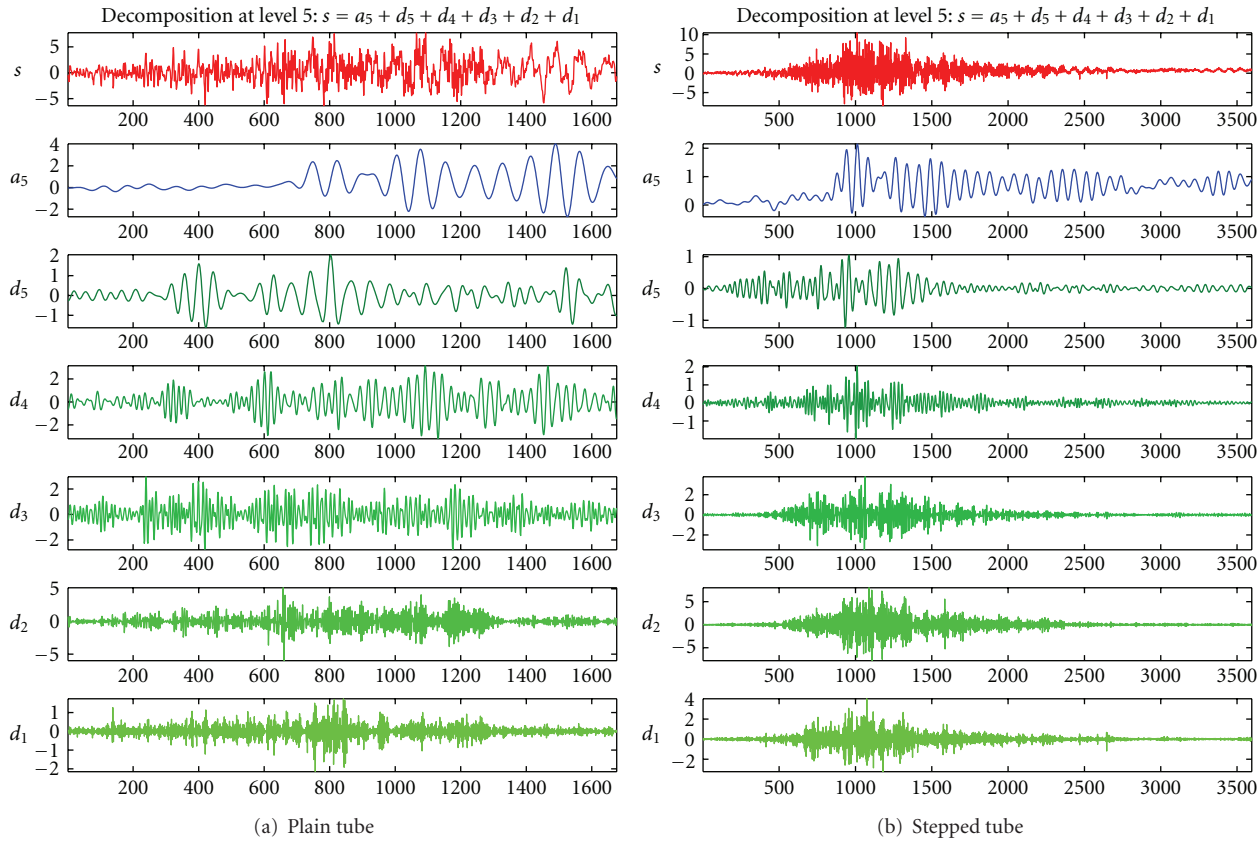

Figure 24: Strain signal decomposition at location number 8.

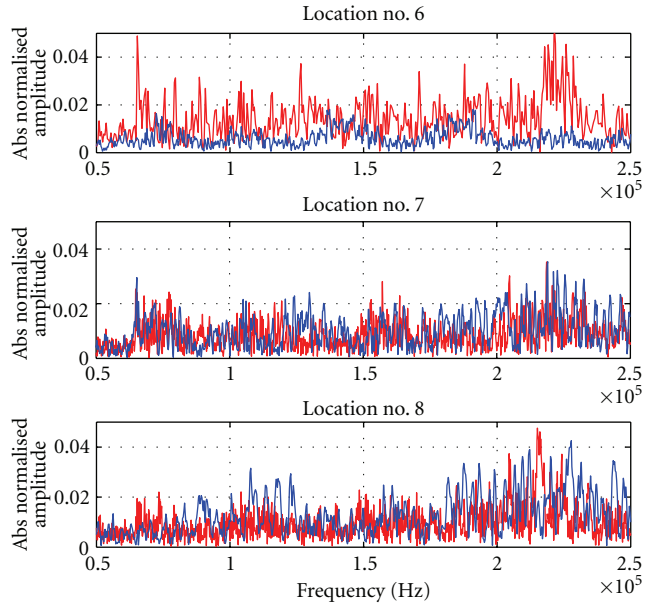

Figure 25: Frequency domain analysis at locations numbers 6, 7, and 8, red color for original and blue color for stepped tube.

high-accuracy pointing precision although it is considered as an antinode point. Figures 30(a) and 30(b) illustrate the bullet position in the shell versus the normalized displacement, for plain and stiffened tube. The figure shows that the shell response to the bullet is delayed until the bullet reaches about 50% of the shell tube length and the maximum deflection is reduced from 0.33 to 0.175 by a ratio of 47%.

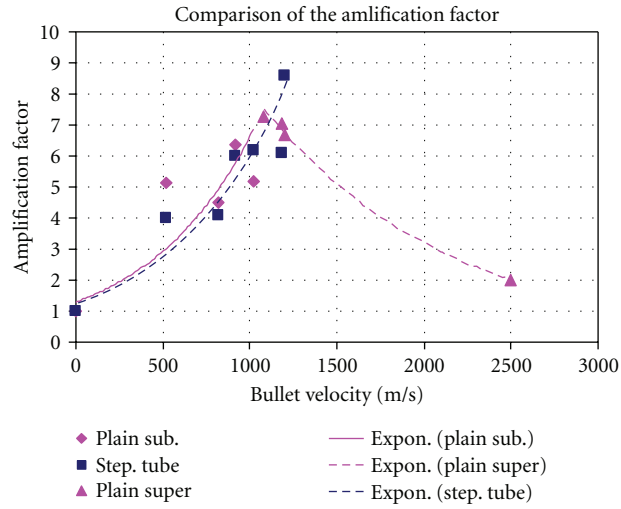

Figure 26: Amplification factor.

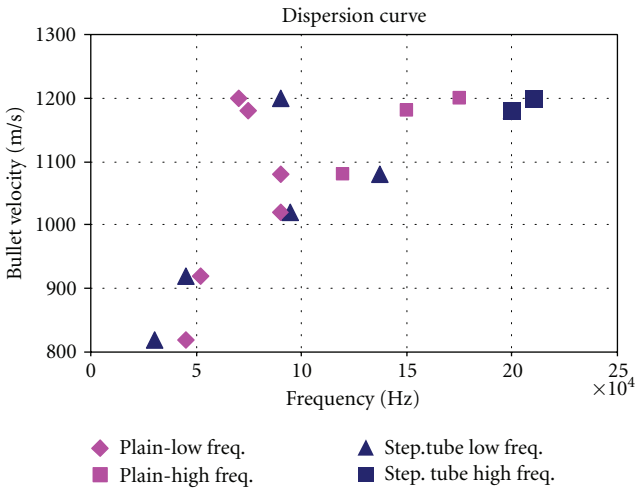

Figure 27: The dispersion curve.

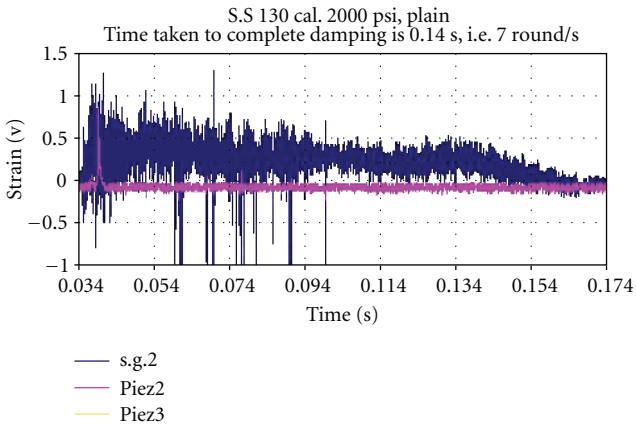

Figure 28: The radial-bending vibrations of plain tube.

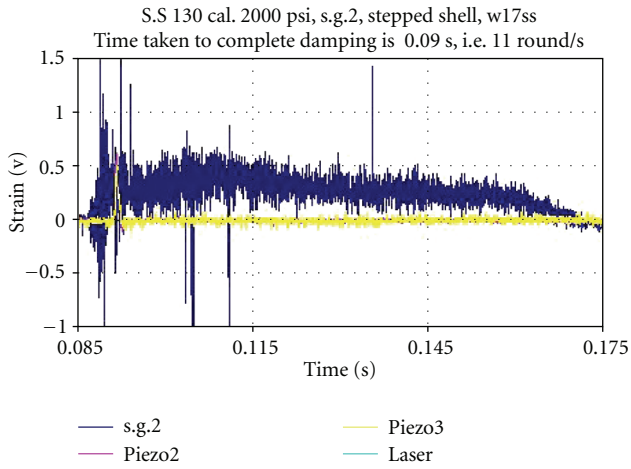

Figure 29: The radial-bending vibrations of the stiffened tube.

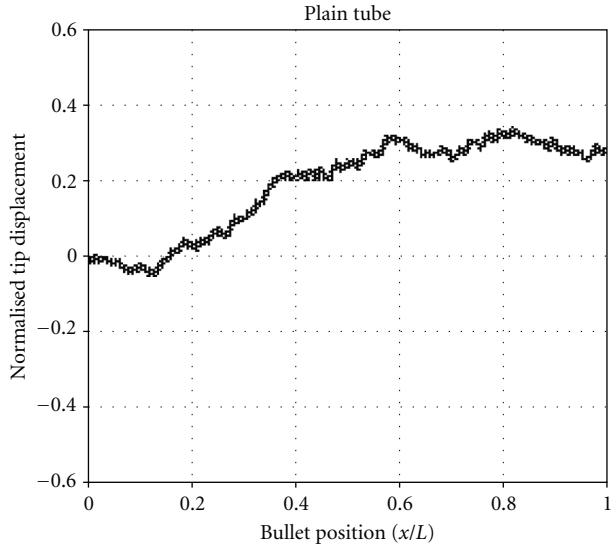

(a) Plain Tube

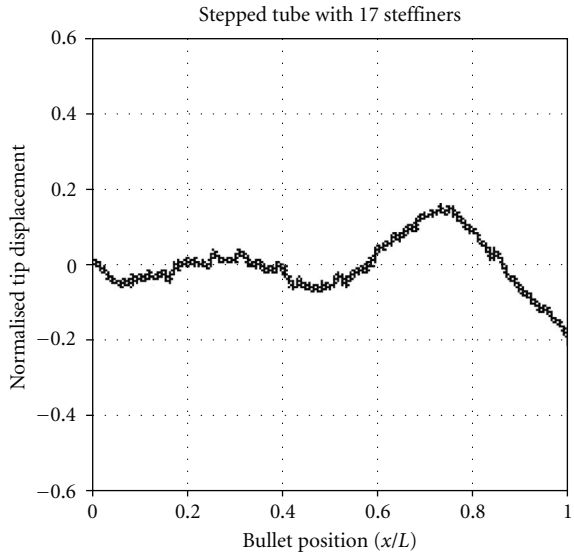

(b) Stiffened tube

Figure 30: Output signals at location number 2.

4. Conclusion

The load acting on a cylindrical shell, with added periodic stiffeners, under a transient pressure pulse propelling a pullet has been experimentally studied.

The study comprises of two modes of velocity, the first is subcritical velocity mode and the second is the supercritical velocity mode. The measured time domain strain signals have been analyzed in order to get the frequency domain modes of vibration using "wavelet transform (WT) package" instead of "fast Fourier transform (FFT)," the package is found to be very powerful, and the decomposition of the signals by this way gave us a clear and good knowledge about the phenomena that we are looking for.

Adding periodic stiffeners has a significant effect on the damping of the shell vibrations; it reaches to values between 38 and 75% for subcritical and critical velocity modes. The critical frequency of the stiffened shell is increased to about the running velocity, so the supercritical mode is changed to subcritical.

The critical velocity of the stiffened tube is increased to about 1190 m/s and the critical frequency is increased to about 200 kHz, by ratios of about 113.9% and 174.5%, respectively, when adding stiffeners which have a mass ratio of 5.6% of the mass of the plain tube.

The amplification and dispersion factors are determined and constructed; they indicated that the corresponding speed and frequencies are shifted to lower values by about 10%, less than that plain tube for subcritical velocity modes.

The radial-bending vibrations and tube muzzle motions are detected at muzzle velocity ratio of 0.99%; the results indicated that there is a possibility of significant increase in the number of rounds per second by about 36% and also increasing the pointing precision by about 47%.

Acknowledgments

This experimental work is done under the supervision of Prof. Dr. Amr Baz during the author's work as a Research Associate in University of Maryland at College Park, USA (2000–2002). This work is funded by The US Army Research Office (Grant no. DAAD199910200). Special thanks are due to Dr. Gary Anderson, the Technical Monitor, for his invaluable technical inputs.

References

[1] L. Fryba, *Vibration of Solids and Structures Under Moving Loads*, Noordhoff, Groningen, The Netherlands, 1977.

[2] D. F. Finlayson, "Characterization of the dynamic strain excitation force in gun tubes," in *Proceedings of the 9th Symposium of Gun Dynamics (SAVIAC '00)*, pp. 12.1–12.16, Baltimore, Md, USA, November 2000.

[3] T. E. Simkins, "Amplification of flexural waves in gun tubes," *Journal of Sound and Vibration*, vol. 172, no. 2, pp. 145–154, 1994.

[4] T. E. Simkins, G. A. Pflegl, and E. G. Stilson, "Dynamic strains in a 60 mm gun tube: an experimental study," *Journal of Sound and Vibration*, vol. 168, no. 3, pp. 549–557, 1993.

[5] W. M. Beltman, E. N. Burcsu, J. E. Shepherd, and L. Zuhal, "The structural response of cylindrical shells to internal shock loading," *Journal of Pressure Vessel Technology*, vol. 121, no. 3, pp. 315–322, 1999.

[6] G. O. Thomas, "The response of pipes and supports to internal pressure loads generated by gaseous detonations," *Journal of Pressure Vessel Technology*, vol. 124, no. 1, pp. 66–73, 2002.

[7] A. Baz, K. Saadeldin, and A. A. Elzahaby, "The structural response of cylindrical shells under internal moving pressure and mass," in *Proceedings of the 11th International Conference On Applied Mechanics and Mechanical Engineering (AMME '04)*, Military Technical College, Kobry Elkobbah, Cairo, Egypt, May 2004.

[8] M. Abu-Hilal and M. Mohsen, "Vibration of beams with general boundary conditions due to a moving harmonic load," *Journal of Sound and Vibration*, vol. 232, no. 4, pp. 703–717, 2000.

[9] Y.-H. Lin and M. W. Trethewey, "Finite element analysis of elastic beams subjected to moving dynamic loads," *Journal of Sound and Vibration*, vol. 136, no. 2, pp. 323–342, 1990.

[10] H. D. Nelson and R. A. Conover, "Dynamic stability of a beam carrying moving masses," *Journal of Applied Mechanics*, vol. 38, no. 4, pp. 1003–1006, 1971.

[11] C. R. Steele, "The finite beam with a moving load," *Journal of Applied Mechanics*, vol. 34, pp. 111–488, 1967.

[12] C. R. Steele, "The timoshenko beam with a moving load," *Journal of Applied Mechanics*, vol. 40, pp. 481–488, 1973.

[13] V. V. Bolotin, *The Dynamic Stability of Elastic Systems*, Holden Day, San Francisco, Calif, USA, 1964.

[14] M. Ruzzene and A. Baz, "Dynamic stability of periodic shells with moving loads," *Journal of Sound and Vibration*, vol. 296, no. 4-5, pp. 830–844, 2006.

[15] M. Ruzzene and A. Baz, "Response of periodically stiffened shells to a moving projectile propelled by an internal pressure wave," *Mechanics of Advanced Materials and Structures*, vol. 13, no. 3, pp. 267–284, 2006.

[16] O. J. Aldraihem and A. Baz, "Moving-loads-induced instability in stepped tubes," *Journal of Vibration and Control*, vol. 10, no. 1, pp. 3–23, 2004.

[17] O. J. Aldraihem and A. Baz, "Dynamic stability of stepped beams under moving loads," *Journal of Sound and Vibration*, vol. 250, no. 5, pp. 835–848, 2002.

[18] R. D. Blevins, *Formulas for Natural Frequency and Mode Shapes*, Krieger, 1995.

[19] M. L. Baron and H. H. Bleich, "Tables of frequencies and mode shapes of infinitely long thin cylindrical shells," *Journal of Applied Mechanics*, vol. 76, pp. 178–184, 1954.

[20] H. H. Bleich and M. L. Baron, "Free and long vibrations of an infinitely long cylindrical shell in an infinite acoustic medium," *Journal of Applied Mechanics*, vol. 19, pp. 167–176, 1954.

[21] S. Tang, "Dynamic response of a tube under moving pressure," *ASCE: Journal of the Engineering Mechanics*, vol. 91, no. 5, pp. 97–121, 1965.

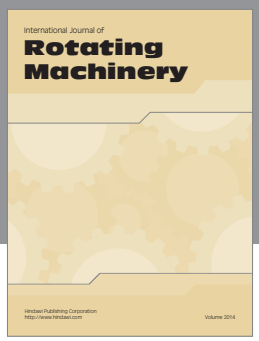

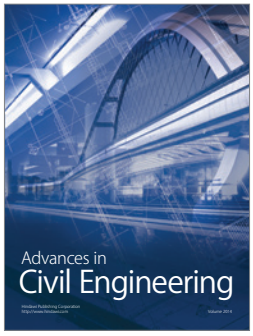

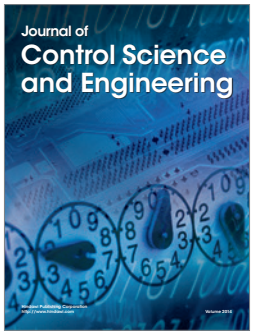

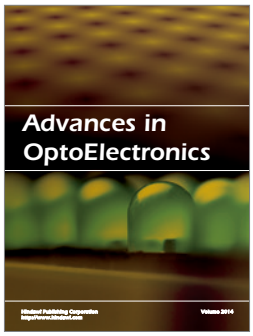

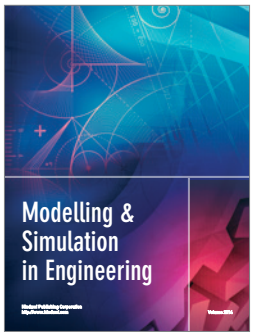

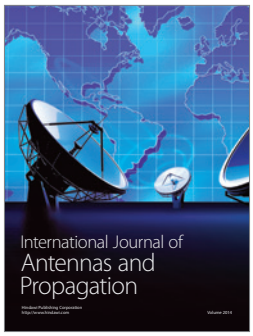

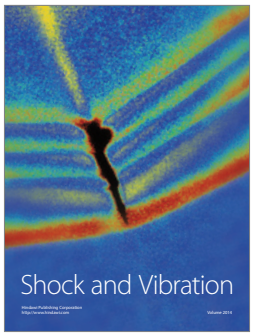

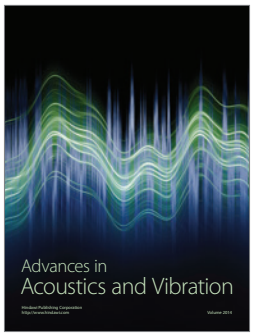

Hindawi

Submit your manuscripts at
http://www.hindawi.com